JACS
JOURNAL OF THE AMERICAN CHEMICAL SOCIETY

ARTICLE

pubs.acs.org/JACS

Impact of Water on the OH + HOCl Reaction

Javier Gonzalez,[†] Josep M. Anglada,[*,†] Robert J. Buszek,[‡] and Joseph S. Francisco[*,‡]

[†]Institut de Quimica Avançada de Catalunya Departament de Quimica Biologica I Modelitzacio Molecular IQAC-CSIC, E-08034 Barcelona, Spain

[‡]Department of Chemistry and Department of Earth and Atmospheric Science, Purdue University, West Lafayette, Indiana 46907

Supporting Information

ABSTRACT: The effect of a single water molecule on the OH + HOCl reaction has been investigated. The naked reaction, the reaction without water, has two elementary reaction paths, depending on how the hydroxyl radical approaches the HOCl molecule. In both cases, the reaction begins with the formation of prereactive hydrogen bond complexes before the abstraction of the hydrogen by the hydroxyl radical. When water is added, the products of the reaction do not change, and the reaction becomes quite complex yielding six different reaction paths. Interestingly, a geometrical rearrangement occurs in the prereactive hydrogen bonded region, which prepares the HOCl moiety to react with the hydroxyl radical. The rate constant for the reaction without water is computed to be 2.2×10^{-13} cm^3 molecule^{-1} s^{-1} at room temperature, which is in good agreement with experimental values. The reaction between ClOH···H_2O and OH is estimated to be slower than the naked reaction by 4−5 orders of magnitude. Although, the reaction between ClOH and the H_2O···HO complex is also predicted to be slower, it is up to 2.2 times faster than the naked reaction at altitudes below 6 km. Another intriguing finding of this work is an interesting three-body interchange reaction that can occur, that is HOCl + HO···H_2O → HOCl···H_2O + OH.

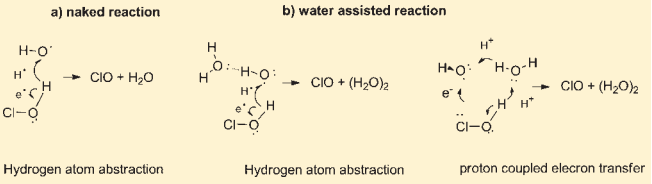

1. INTRODUCTION

Hypochlorous acid, HOCl, is a temporary reservoir for ClO_x (i.e., Cl or ClO) species in the atmosphere, particularly the stratosphere.[1−4] The photolysis of HOCl is a key reaction in the catalytic depletion of ozone, a cycle that couples both the HO_x and the ClO_x cycles. For example, Soloman et al.[5] proposed that the dominant catalytic ozone loss involving HO_x and ClO_x radicals is as follows:

$$Cl + O_3 \rightarrow ClO + O_2$$

$$OH + O_3 \rightarrow HO_2 + O_2$$

$$HO_2 + ClO \rightarrow HOCl + O_2$$

$$HOCl + h\nu \rightarrow Cl + OH$$

$$\text{Net}: 2O_3 \rightarrow 3O_2$$

This cycle is thought to be responsible for 30% of the loss of ozone by chlorine.[6] HOCl is readily photolyzed at wavelengths shorter than 420 nm to regenerate Cl and OH radicals. The photolysis of HOCl also plays an integral role in a more recent proposal of ozone destruction involving ClO dimer:[7,8]

$$ClO + ClO + M \rightarrow ClOOCl + M$$

$$OH + ClOOCl \rightarrow HOCl + ClOO$$

$$ClOO + M \rightarrow Cl + O_2 + M$$

$$HOCl + h\nu \rightarrow OH + Cl$$

$$2(Cl + O_3 \rightarrow ClO + O_2)$$

$$\text{Net}: 2O_3 \rightarrow 3O_2$$

Photolysis of HOCl is present in these catalytic cycles because it quickly reactivates Cl, which is then free to destroy ozone. An alternate reaction for HOCl is the reactivation of ClO radicals via reaction with OH radicals:

$$OH + HOCl \rightarrow ClO + H_2O$$

However, this reaction is known to be slow. Ennis and Birks[9] reported the rate constant to be $1.7 \times 10^{-13} - 9.5 \times 10^{-13}$ cm^3 molecule^{-1} s^{-1} at room temperature. Atkinson et al.[10] recommended the following rate for the OH + HOCl reaction, $k(OH + HOCl) = 3.01 \times 10^{-12} \exp(-4.16/RT)$ cm^3 molecule^{-1} s^{-1}. The theoretical study of Wang et al.[11] and Xu et al.[12] also support a slow rate for the OH + HOCl reaction.

In some of the recent literature, water has been shown to drastically change the potential energy surfaces of radical−molecule reactions. Vöhringer−Martinez et al.[13] is one of the first studies to demonstrate

Received: February 3, 2010
Published: February 14, 2011

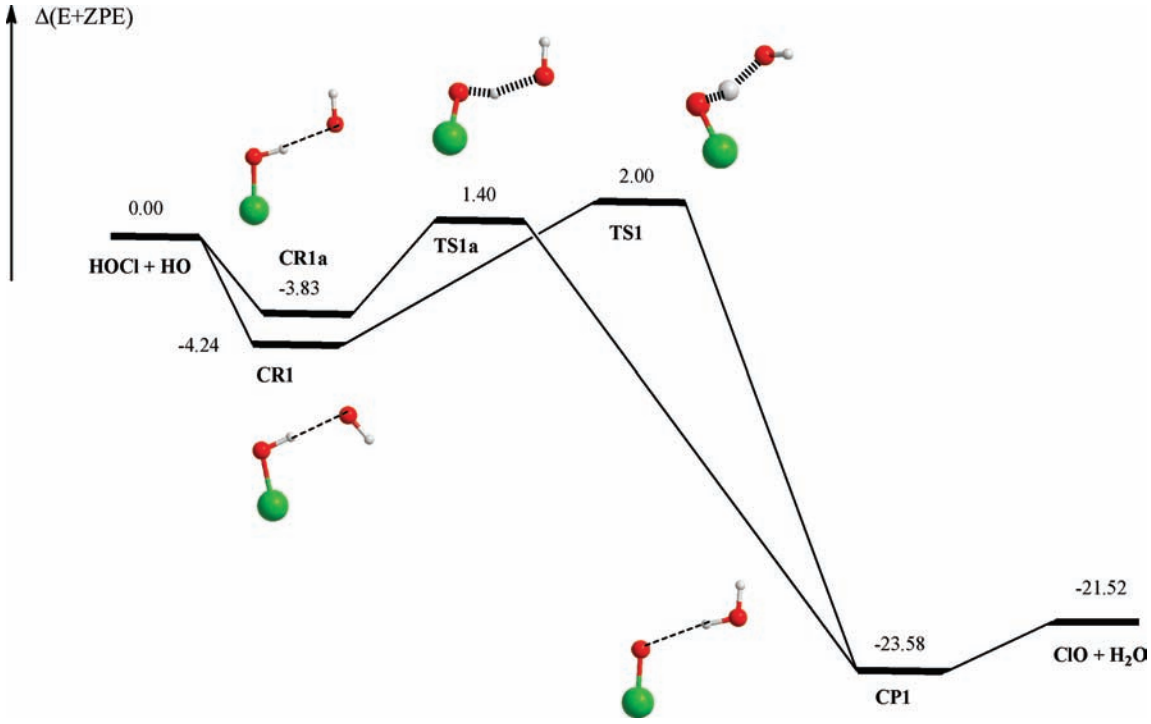

Figure 1. Schematic energy diagram for the reaction between HOCl and OH.

how a single water molecule can catalyze a radical−molecule reaction involving OH radical. New studies are showing how reactions of formic acid[14,15] and trifluoromethanol[16] are impacted by water. The present work investigates the possible role of water as a catalyst, via altering the energetic reaction barriers and therefore the kinetics, for the OH + HOCl reaction and its relevance in the atmosphere. In particular, this study focuses on the effect of a single water on the OH + HOCl reaction.

2. COMPUTATIONAL DETAILS

All calculations have been carried out employing the aug-cc-pVTZ basis set.[17,18] All stationary points in the potential energy surface have been fully optimized with the hybrid density functional B3LYP method.[19] Harmonic vibrational frequencies have also been calculated using B3LYP to verify the nature of the corresponding stationary point (minima or transition state), to provide the zero point vibrational energy (ZPE) and the thermodynamic contributions to the enthalpy and free energy. Moreover, intrinsic reaction coordinate (IRC)[20,21] calculations have been done to ensure that a given transition state connects with the desired minima. The final energies are obtained by performing CCSD(T)[22−24] single-point energy calculations at the geometries optimized with the B3LYP approach. For the reaction without water, all stationary points have been optimized using the CASSCF method, along with single-point energy calculations at CASPT2 to account for the dynamical correlation energy. The active space for these calculations consists of 13 electrons over 13 orbitals; this is chosen according the fractional occupation of the natural orbitals obtained from a multireference configuration interaction wave function considering all valence electrons.[25]

For several stationary points of interest, the bonding features are also calculated using the atoms in molecules (AIM) theory by Bader.[26] Finally, the kinetic properties of the system are calculated employing conventional transition state theory (TST). These calculations make use of the energies obtained at the CCSD(T)/aug-cc-pVTZ//B3LYP/aug-cc-pVTZ level and the partition functions computed at the B3LYP/aug-cc-pVTZ level of theory. The tunnelling correction to the rate constants have been considered and computed by the zero-order approximation to the vibrationally adiabatic PES with zero curvature. In this case, the unsymmetrical Eckart potential energy barrier is used to approximate the potential energy curve.[27]

The geometry optimizations at B3LYP level of theory and the CCSD(T) single-point energy calculations have been done with the *Gaussian03* suite of programs.[28] The CASSCF and CASPT2 calculations have been carried out using the *MOLCAS 7.4* program.[29] TST rate constants and tunnelling corrections have been computed using the *Polyrate* program.[30] The topological properties of the wave function are obtained with the *AIMPAC* program package.[31] The *Molden* program[32] is also used to visualize the geometrical and electronic features of the different stationary points.

3. RESULTS AND DISCUSSION

The different transition states are named by the prefix **TS** followed by a number; a letter **a** is added to distinguish those transitions states that are conformers of one other and therefore having the same features. The prereactive and postreactive complexes of a given elementary reaction are named by adding the prefixes **CR** and **CP**, respectively. The most relevant geometrical parameters of all stationary points described in this work have been drawn in Figure S1 of the Supporting Information.

3.1. Potential Energy Surfaces of the OH + HOCl Reaction without and with Water. Two theoretical studies have been reported recently for the reaction without water.[11,12] In this study, we have found two elementary reaction paths depending on how the hydroxyl radical approaches HOCl, corresponding to the cis and trans orientation of the two HOCl and OH moieties. A schematic representation of the corresponding potential energy surfaces (PES) can be seen in Figure 1; Table 1 contains the zero point energy (ZPE), relative energies, enthalpies, and free energies at 298 K for the corresponding stationary points. As usual in many atmospheric gas-phase reactions involving

dx.doi.org/10.1021/ja100976b |*J. Am. Chem. Soc.* 2011, 133, 3345–3353

hydroxyl radicals, each elementary reaction begins with the formation of prereactive hydrogen bonded complexes (**CR1** and **CR1a**) before the transition states and the formation of the products. Both prereactive complexes are held by a hydrogen bond interaction between the hydrogen atom of the HOCl and the oxygen atom of the hydroxyl radical. **CR1** and **CR1a** have a planar structure and lie in electronic state X^2A''; the unpaired electron is primarily localized over the oxygen atom of the hydroxyl radical moiety, perpendicular to the molecular symmetry plane. Table 1 and Figure 1 shows a binding energy of 4.24 and 3.83 kcal mol^{-1} for **CR1** and **CR1a**, respectively. The reaction proceeds through transition states **TS1** and **TS1a** forming the postreactive complex **CP1**, before the release of the products, ClO and H_2O. **CP1** also has a planar structure ($^2A''$ electronic state) and is stabilized by a hydrogen bond interaction between the oxygen atom of the ClO radical and one hydrogen atom of water. The analysis of the wave function at the two transition states indicates that the reaction involves the concerted breaking and forming of the (Cl)O−H and H−O(H) bond.

Table 1. Zero Point Energy (ZPE, in kcal mol^{-1}), Entropies (S in e.u.), and Relative Energies (ΔE and Δ(E+ZPE) in kcal mol^{-1}), Enthalpies ($\Delta H(298)$ in kcal mol^{-1}), and Free Energies ($\Delta G(298)$ in kcal mol^{-1}) for the HOCl + HO Reaction[a]

system	ZPE	ΔE	Δ (E+ZPE)[b]	$\Delta H(298)$	$\Delta G(298)$
HOCl + HO	13.5	0.00	0.00	0.00	0.00
Cr1	14.8	−5.52	−4.24	−4.48	1.70
TS1	13.2	2.30	2.00	0.94	9.46
Cr1a	14.7	−5.00	−3.83	−4.06	2.33
TS1a	13.7	1.25	1.40	0.35	8.83
Cp1	15.6	−25.70	−23.58	−23.68	−18.01
ClO + H_2O	14.55	−22.55	−21.52	−21.55	−21.20

[a] ZPE and S values obtained at B3LYP/aug-cc-pVTZ level of theory. The energy values are obtained at CCSD(T)/aug-cc-pVTZ//B3LYP/aug-cc-pVTZ level of theory whereas the *H* and *G* corrections are taken from the B3LYP/aug-cc-pVTZ values. [b] The computed CASPT2/aug-cc-pVTZ //CASSCF(13,13)/aug-cc-pVTZ relative energies (Δ(E+ZPE) values in kcal/mol) are: −5.36 for **Cr1**; −4.88 for **Cr1a**; 0.90 for **TS1**; 1.07 for **TS1a**; and −22.43 for the reaction energy (ClO + H_2O).

This process has been indicated in part a of Scheme 1 and corresponds to the *conventional hydrogen abstraction radical type mechanism* (HAT). Thus, starting from the prereactive complexes (having a π electronic structure) the hydroxyl radical moiety must rotate along the reaction path to allow the unpaired electron to interact with the (Cl)O−H bond and abstract the hydrogen.

From an energetic point of view, Figure 1 and Table 1 show that the two transition states **TS1** and **TS1a** are predicted to lie at 2.00 and 1.40 kcal mol^{-1} at 0 K respectively above the energy of the separate reactants, whereas **CP1** is predicted to lie 23.58 kcal mol^{-1} below the reactants. The energetic values for **CR1**, **TS1**, and **CP1** compare quite well with results from the literature.[11,12] At 0 K the reaction energy is computed to be −21.52 kcal mol^{-1} and the ΔH_f^0 is predicted to be −21.55 kcal mol^{-1}, compared with the experimental estimates of −24.9 kcal mol^{-1}.[33−36] To check the reliability of our calculations, CASSCF geometry optimizations and CASPT2 single-point energy calculations are carried out for the reactants, products, prereactive complexes, and transition states and the results are contained in footnote b of Table 1. The results show that the energy barriers of the transition states, relative to the prereactive complexes, agree with those obtained at CCSD(T) level of theory, with differences between 0.02 and 0.72 kcal mol^{-1}, whereas the reaction energy differs by 0.91 kcal mol^{-1} with the value predicted at CCSD(T) level of theory.

The influence of a single water molecular on the HOCl + OH reaction has been investigated by taking into account that (a) HOCl forms a hydrogen bonded complex with water and subsequently reacts with OH radical and (b) HOCl reacts with a previously formed HO···H_2O complex. For the HOCl···H_2O reactant two different complexes are found (*cis*- and *trans*-HOCl···H_2O) that have been previously reported in the literature, the findings here predict them to have a binding energy of 5.91 and 5.63 kcal mol^{-1} respectively, which is in good agreement with previously reported values.[37] For the HO···H_2O complex, the computed binding energy is 3.82 kcal mol^{-1}, also in good agreement with results from the literature.[38−41]

Starting from both the (a) and (b) reactant channels, the same products as the naked reaction are obtained, but the potential energy surface appears to be much more complex and the reaction becomes more versatile. Figure 2 shows a schematic

Scheme 1. Pictorial Representation of the Electronic Features of the ClOH + OH Reaction without and with Water

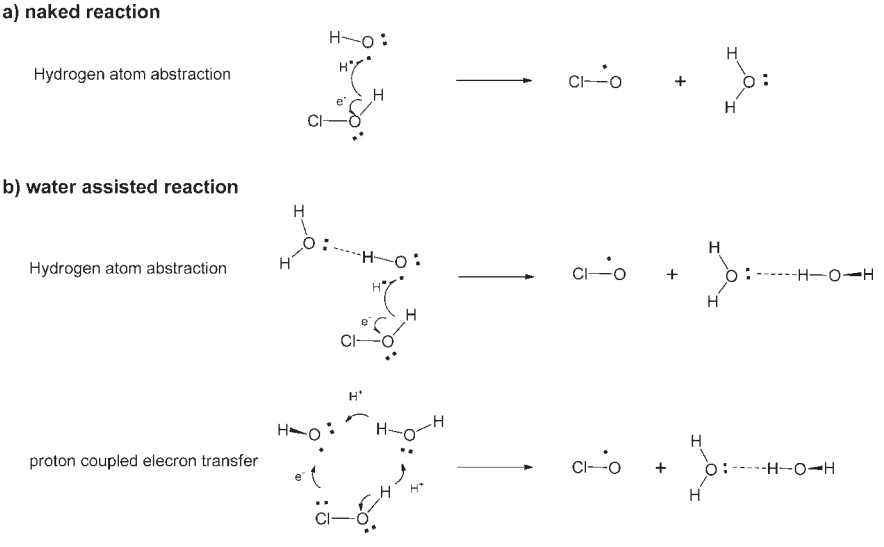

dx.doi.org/10.1021/ja100976b |*J. Am. Chem. Soc.* 2011, 133, 3345–3353

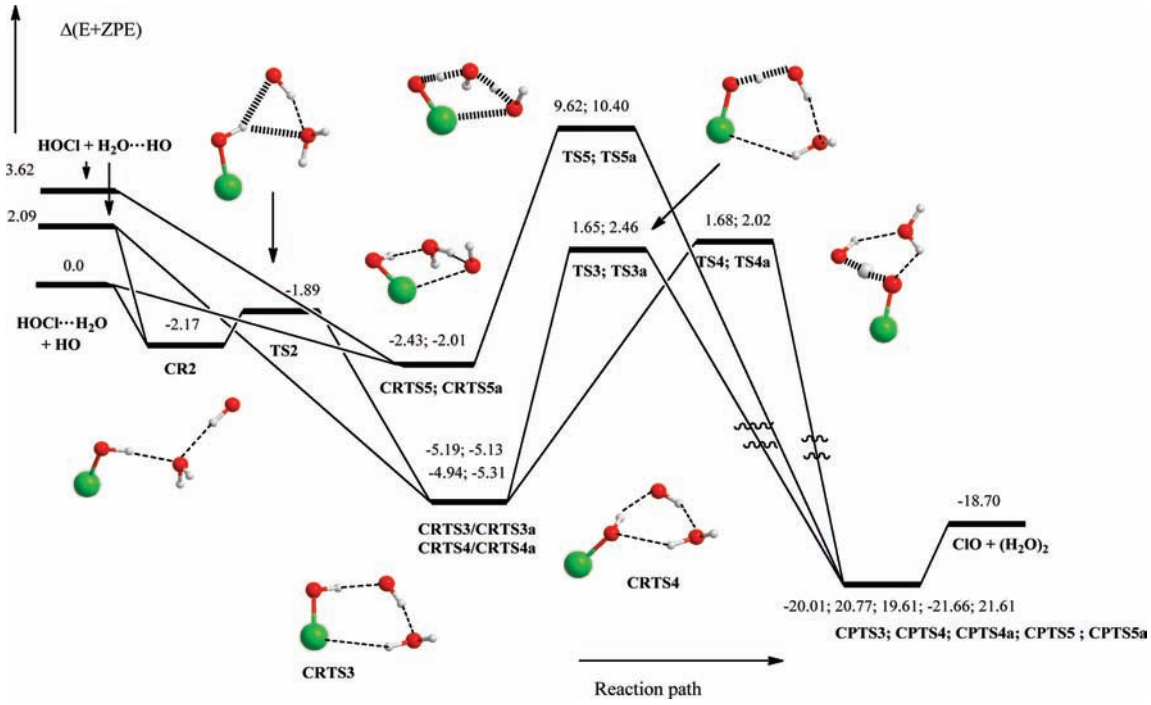

Figure 2. Schematic energy diagram for the water-assisted reaction between HOCl and OH.

potential energy surface, pointing out the existence of six different reaction paths. Table 2 contains the zero point energy (ZPE), relative energies, enthalpies, and free energies at 298 K for the corresponding stationary points. These six different reaction paths are labeled as **TS3**; **TS3a**; **TS4**; **TS4a**; **TS5**; and **TS5a**. The suffix **a** is added to distinguish between those stationary points being conformers of each other, differing only in the orientation of the one of the hydrogen atoms of the water molecule.

Similar to the naked reaction described above, each reaction begins with the formation of a prereactive hydrogen bond complex, but now the prereactive region is much more complex and changes in this region can potentially change the reactivity. Figure 2 shows that, beginning with the $ClOH\cdots H_2O$ + OH reactants, the first step of the reaction involves the formation of the **CR2** hydrogen bond complex, in which the hydroxyl radical interacts with the lone pair of the water molecule of the $ClOH\cdots H_2O$ reactant. Thus, the **CR2** complex is formed by three moieties, which are held together by two hydrogen bonds ($ClOH\cdots H_2O\cdots HO$) with a computed binding energy of 2.17 kcal mol^{-1}. After the transition state, **TS2**, which has an energy barrier of only 0.28 kcal mol^{-1}, relative to **CR2**, lying below the energy of the reactants, the seven-member ring **CRTS3** hydrogen bonded complex is formed, with a binding energy of 5.19 kcal mol^{-1}. Figure 2 shows that **CRTS3** has three hydrogen bonds, the first between the hydrogen atom of the HOCl moiety and the oxygen atom of the hydroxyl radical moiety; the second one between the hydrogen atom of the OH moiety and the oxygen atom of water and the third one between one hydrogen atom of water and the chlorine atom. Please note that an important structural change has occurred in this step. In **CR2**, and in the $ClOH\cdots H_2O$ reactant, the hydrogen atom of the hypochlorous acid moiety interacts with the oxygen of water, which hampers the ability for hydrogen to be abstracted by the hydroxyl radical. However, in **CR3** the hydrogen atom of the HOCl moiety interacts with the oxygen of the hydroxyl radical so that it is able to react. Although not shown in Figure 2, **CRTS3** is connected to the **CRTS4** complex through the transition state **TS6S**, having a very low energy barrier, 0.11 kcal mol^{-1} relative to **CRTS3**, as seen in Table 2 and in the Supporting Information. **CRTS4** has a six-member ring structure differing from **CRTS3** in the third hydrogen bond, which is now formed between one hydrogen atom of water and the oxygen atom of the HOCl moiety and has a computed binding energy of 4.94 kcal mol^{-1}. The low energy barrier connecting these hydrogen bond complexes assures that both will be populated. **CRTS3a** and **CRTS4a** have the same features as **CRTS3** and **CRTS4**, respectively (Figure 2, Table 2, and the Supporting Information) and their binding energies differ by at most in 0.37 kcal mol^{-1} relative to the discussed complexes.

After these prereactive complexes the reaction goes on through four different elementary reactions (**TS3**, **TS3a**, **TS4**, and **TS4a**) and these transition states lay 1.65, 2.46, 1.68, and 2.02 kcal mol^{-1} respectively above the reactants. All of these elementary processes involve a *conventional hydrogen abstraction radical type mechanism* similar to the reaction without water, as described above (part b of Scheme 1). These transition states differentiate from one another in the relative orientation of the $OH\cdots H_2O$ and HOCl moieties as described for the prereactive complexes. **TS3**, for instance, is stabilized by two hydrogen bonds; the first one between the hydrogen of the hydroxyl radical moiety and the oxygen of water and the second one between one hydrogen atom from water and the chlorine atom; whereas in **TS4** the second hydrogen bond occurs between on hydrogen of water and the oxygen atom of the ClO moiety. In the exit channel, postreactive complexes (**CPTS3**, **CPTS4**, **CPTS4a**) are formed for each elementary reaction whose binding energies lie between 19.61 and 20.77 kcal mol^{-1} below the reactants.

Beyond the reaction paths described above, two additional elementary reactions are found. Beginning with the prereactive complexes **CR5** and **CR5a**, and going through transition states **TS5** and

dx.doi.org/10.1021/ja100976b |*J. Am. Chem. Soc.* 2011, 133, 3345–3353

Table 2. Zero Point Energy (ZPE, in kcal mol^{-1}), Entropies (S in e.u.), and Relative Energies (ΔE and Δ(E+ZPE) in kcal mol^{-1}), Enthalpies ($\Delta H(298)$ in kcal mol^{-1}), and Free Energies ($\Delta G(298)$ in kcal mol^{-1}) for the Reaction with a Single Water Molecule[a]

compound	ZPE	S	ΔE	Δ-(E+ZPE)	ΔH-(298)	ΔG-(298)
HOCl···H_2O + HO	28.9	120.4	0.00	0.00	0.00	0.00
HOCl + H_2O···HO	28.9	123.2	2.09	2.09	1.77	0.95
HOCl + HO···H_2O	28.2	126.6	4.31	3.62	3.68	1.84
CR2	30.54	97.04	−3.80	−2.17	−2.53	4.43
TS2	29.83	92.99	−2.82	−1.89	−2.49	5.69
CRTS3	30.84	90.0	−7.12	−5.19	−6.02	3.05
TS3	27.96	88.1	2.59	1.65	0.52	10.16
CRTS3a	30.78	91.8	−7.01	−5.13	−5.89	2.63
TS3a	27.86	89.3	3.50	2.46	1.42	10.68
CPTS3	30.63	103.2	−21.74	−20.01	−19.80	−14.67
CRTS4	31.0	89.9	−7.03	−4.94	−5.81	3.28
TS4	28.16	89.1	2.42	1.68	0.61	9.93
CPTS4	30.64	103.4	−22.50	−20.77	−20.56	−15.50
CRTS4a	30.9	91.4	−7.28	−5.31	−6.10	2.54
TS4a	27.98	93.9	2.95	2.02	1.15	9.33
CPTS4a	30.63	103.4	−21.34	−19.61	−19.40	−14.34
CRTS5	31.66	84.8	−5.19	−2.43	−3.69	6.91
TS5	28.48	78.0	10.05	9.62	7.39	20.03
CPTS5	31.12	97.9	−23.88	−21.66	−21.85	−15.15
CRTS5a	31.62	84.9	−4.72	−2.01	−3.24	7.33
TS5a	28.49	77.8	10.81	10.40	8.15	20.84
CPTS5a	31.12	97.9	−23.83	−21.61	−21.80	−15.10
TS6S	30.55	88.6	−6.72	−5.07	−6.16	3.32
ClO + $(H_2O)_2$	30.0	122.5	−19.80	−18.70	−18.84	−19.45
ClO + $2H_2O$	27.9	143.0	−14.58	−15.61	−15.26	−22.00

[a] ZPE and S values obtained at the B3LYP/aug-cc-pVTZ level of theory. The energy values are obtained at the CCSD(T)/aug-cc-pVTZ//B3LYP/aug-cc-pVTZ level of theory, whereas the H and G corrections are taken from the B3LYP/aug-cc-pVTZ values. H_2O···HO is the global minimum of the water hydroxyl radical complex. HO···H_2O is a local minimum of the water hydroxyl radical complex.

TS5a to form post reactive complexes **CP5** and **CP5a**, respectively. The transition states for these elementary reactions have very high energy barriers (**TS5** and **TS5a** are computed to lie 9.62 and 10.40 kcal mol^{-1} above the HOCl···H_2O + OH reactants). Hence, neither of these reactions will be of any atmospheric relevance. These processes are only noted as they have very interesting electronic features, involving the transfer of an electron from the chlorine atom to the oxygen atom of the hydroxyl radical and, simultaneously, a double-proton transfer, from the HOCl to water and from water to the OH moiety. This corresponds to *a proton coupled electron transfer mechanism* (also part b of Scheme 1) and points out that the chlorine atom can also participate in similar mechanisms as the oxygen atom.[15,42,43]Figure 2 also shows that, starting from the HOCl + H_2O···HO reactants, the reaction can proceed through all the same elementary reactions as described above, although in this case, the entrance channel lies 2.09 kcal mol^{-1} above the HOCl···H_2O + OH channel.

Finally, it is of interest to know how additional water molecules will effect the reaction and therefore the reaction between HOCl and the $(H_2O)_2$···HO cluster is also investigated. The corresponding schematic potential energy surface is drawn in Figure 3, which shows the existence of seven different elementary reaction paths. The transition states labeled as **TS6**, **TS6a**, **TS6b**, **TS7**, **TS7a**, **TS8**, and **TS9**; once again, those having a small letter as a suffix are isomers that differentiate to each other only in the relative orientation of the dangling hydrogen atoms, however only the most stable conformer will be discussed. The Supporting Information contains the most relevant geometrical parameters and the relative energies, ZPE values, relative enthalpies, and free energies. The reaction path having the lowest energy occurs through **TS6**. It begins with the formation of the prereactive complex **CRTS6**, which has an eight-membered ring structure. Figure 3 shows that **CR6** has a binding energy close to 10 kcal mol^{-1} relative to the HOCl + $(H_2O)_2$···HO reactants and the transition state lies 3.03 kcal mol^{-1} below the energy of the separate reactants. Comparing this result with those reported above for the reaction between HOCl and H_2O···HO described above (Figure 2, Table 2), we conclude that the inclusion of a second water molecule produces a catalytic effect of 2.6 kcal mol^{-1}. The reaction path occurring through **TS7** a involves the interaction of the hydrogen atom of the HOCl with the oxygen atom of the radical complex. It begins with the formation of a prereactive complex **CRTS7 a** having a binding energy of 5.20 kcal mol^{-1}, whereas the transition state lies 0.20 kcal mol^{-1} above the energy of the separate reactants. The reaction paths occurring through **TS8** and **TS9** have higher energy barriers and therefore should not play any role in the reaction. Finally, it is worth mentioning that the reaction energy is computed to be 21.78 kcal mol^{-1} and, in the exit channel, a postreactive hydrogen bonded complex is formed for all elementary reactions before the release of the products (Figure 3). The atmospheric significance of this reaction should be very low because the atmospheric concentration of the $(H_2O)_2$···HO cluster is predicted to be very small, up to 3.48 × 10^2 molecules cm^{-3}.[44] However, the study of this process is important as it brings further molecular insight on how the reaction can take place at a water surface.[45,46]

3.2. Reaction Kinetics. Table 3 shows the rate constants computed under different conditions for the reaction without and with water, more detailed information regarding the different values obtained for each elementary reaction, product distribution for the ClOH + H_2O···HO reaction and equilibrium constants for the formation of the ClOH···H_2O and H_2O···HO complexes can be found in the Supporting Information. The free energy results displayed in Tables 1 and 2 suggest that the prereactive complexes are, in part, shifted to the reactants, so that the rate constant for each process is given by eq 1,

$$k_I = k_{eq} k_2 \quad (1)$$

K_{eq} is the equilibrium constant given by eq 2,

$$K_{eq} = \frac{Q_{CR}}{Q_{R1} Q_{R2}} e^{-(E_{CR} - E_R)/RT} \quad (2)$$

where the various Q denote the partition functions of the reactants and the prereactive complex and E_R and E_{CR} are the corresponding energies. k_2 is the unimolecular rate constant of the elementary reaction going from the prereactive complex to the products.

For the reaction without water, Table 3 shows that the computed value for the rate constant at room temperature is 2.26 × 10^{-13} cm^3 molecule^{-1} s^{-1}, which is in very good agreement with the experimental values.[9] The computed expression of the rate constant is k(OH + HOCl) = 2.4 × 10^{-12} exp (−5.78/RT) cm^3

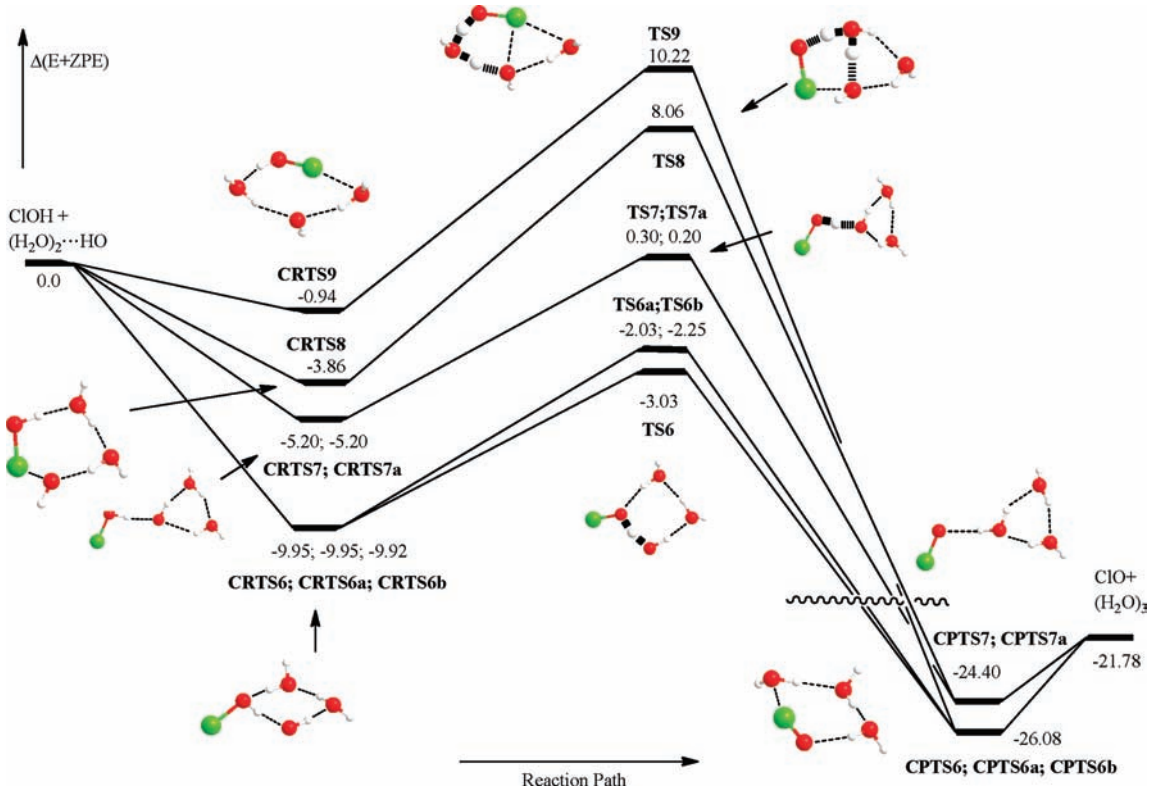

Figure 3. Schematic energy diagram for the reaction between HOCl and the $(H_2O)_2\cdots HO$ cluster.

Table 3. Rate Constants and Effective Rate Constants (in $cm^3 \cdot s^{-1} \cdot molecule^{-1}$) for the ClOH + OH Reaction without and with Water[a] and Water Concentration ($molecule \cdot cm^{-3}$) at Different Heights in the Earth Atmosphere [b]

h (km)	T (K)[c]	k_{v1}	k_{v2}	k_{v3}	$[H_2O]$	k'_{v2}	k'_{v3}	k'_{v2}/k_{v1}	k'_{v3}/k_{v1}
0	298.15	2.26×10^{-13}	1.91×10^{-14}	1.71×10^{-10}	2.59×10^{17}	1.20×10^{-16}	2.49×10^{-13}	5.31×10^{-4}	1.10
0	288.19	1.48×10^{-13}	1.59×10^{-14}	1.79×10^{-10}	2.59×10^{17}	1.36×10^{-16}	3.27×10^{-13}	9.19×10^{-4}	2.21
2	275.21	1.31×10^{-13}	1.20×10^{-14}	1.95×10^{-10}	1.11×10^{17}	6.97×10^{-17}	2.12×10^{-13}	5.32×10^{-4}	1.62
4	262.23	1.15×10^{-13}	8.94×10^{-15}	2.17×10^{-10}	5.38×10^{16}	5.40×10^{-17}	1.63×10^{-13}	4.70×10^{-4}	1.42
6	249.25	9.93×10^{-14}	6.69×10^{-15}	2.45×10^{-10}	1.16×10^{16}	4.24×10^{-17}	5.93×10^{-14}	4.27×10^{-4}	5.97×10^{-1}
8	236.27	8.50×10^{-14}	4.95×10^{-15}	2.81×10^{-10}	3.50×10^{15}	5.06×10^{-18}	3.23×10^{-14}	5.95×10^{-5}	3.80×10^{-1}
10	223.29	7.20×10^{-14}	3.70×10^{-15}	3.33×10^{-10}	9.23×10^{14}	2.05×10^{-18}	1.67×10^{-14}	2.85×10^{-5}	2.32×10^{-1}
12	216.69	6.61×10^{-14}	3.20×10^{-15}	3.65×10^{-10}	2.15×10^{14}	6.15×10^{-19}	5.67×10^{-15}	9.30×10^{-6}	8.57×10^{-2}

[a] k_{v1}, k_{v2}, and k_{v3} are the rate constant for the HOCl + OH, HOCl···H_2O + OH, and HOCl + H_2O···OH reactions, respectively (eqs 4−6). K'_{v2}, and k'_{v3} are the effective rate constants according eqs 5 and 6. [b] Water concentration taken from ref 54. [c] Taken from the NASA atmospheric simulator.[55]

$molecule^{-1}\ s^{-1}$, compared with the expression $k(OH + HOCl) = 3.01 \times 10^{-12} \exp(-4.16/RT)\ cm^3\ molecule^{-1}\ s^{-1}$ recommended by Atkinson et al.[10]

For the reaction with water, Figure 2 shows that the potential energy surface is much more complex, especially in the prereactive hydrogen bonded complex region. As pointed out in the previous section, there are two different reactant channels, the first one involving the interaction between the ClOH···H_2O and OH and the second one involving the reaction between ClOH and the H_2O···HO complex. In the ClOH···H_2O + OH entrance channel, there is a geometrical rearrangement occurring through **CR2** and **TS2**, which prepares the HOCl moiety to react with the hydroxyl radical moiety. The results displayed in Table 2 show that, on the free energy potential energy surface, both **CR2** and **TS2** lie above the reactants and therefore this step is kinetically relevant. Therefore, in this case, k_2 has been calculated according to the canonical unified statistical model described by eq 3.[47,48]

$$\frac{1}{k_2} = \frac{1}{k_{TS2}} + \frac{1}{\sum_{TS3,\,TS3a,\,TS4,\,TS4a} k_{TS}} \qquad (3)$$

Table 3 shows that the computed value for the rate constant at room temperature is $1.91 \times 10^{-14}\ cm^3\ molecule^{-1}\ s^{-1}$, which is almost 12 times smaller than the rate constant for the naked reaction. Moreover, Table 3 also shows that at lower temperatures the rate constant diminishes considerably so that at 223 K the computed value is $3.70 \times 10^{-15}\ cm^3\ molecule^{-1}\ s^{-1}$, which is almost 20 times smaller than the rate constant for reaction without water at the same temperature.

Starting from ClOH + H_2O···HO entrance channel, the first step of the reaction leads directly to the formation of the **CRTS3**

dx.doi.org/10.1021/ja100976b |*J. Am. Chem. Soc.* 2011, 133, 3345–3353

(**CRTS3a**) and **CRTS4** (**CRTS4a**) prereactive complexes and then the reaction can either form ClO + $2H_2O$ (through **TS3** and **TS4**) or ClOH···H_2O + OH (through **TS2** and **CR2**). In this case, the rate constant has been computed according to eq 1, in which k_2 is the sum of the unimolecular rate constants through all of the transition states. The results displayed in Table 3 show that the computed rate constant varies from 3.65×10^{-10} to 1.7×10^{-10} cm^3 $molecule^{-1}$ s^{-1}, in the range of temperatures between 217 and 298 K, respectively. It is interesting to note that the computed branching ratio displayed in the Supporting Information reveals that the ClOH + H_2O···HO reaction produces the ClOH···H_2O + OH product set almost exclusively, at 99.5% (Table S6 of the Supporting Information).

To obtain a more complete knowledge of the effect of water vapor in the ClOH + OH reaction, it is necessary to compare the rate of the naked and water-assisted reactions rather than comparing the rate constants of the individual reactions. The rate for the naked reaction can be written as

$$v_1 = k_{v1}[\mathrm{ClOH}][\mathrm{OH}] \quad (4)$$

whereas the rate for the water-assisted reactions can be written as

$$v_2 = k_{v2}[\mathrm{ClOH}\cdots\mathrm{H_2O}][\mathrm{OH}] = k'_{v2}[\mathrm{ClOH}][\mathrm{OH}] \quad (5)$$

$$v_3 = k_{v3}[\mathrm{OH}\cdots\mathrm{H_2O}][\mathrm{ClOH}] = k'_{v3}[\mathrm{ClOH}][\mathrm{OH}] \quad (6)$$

where $k'_{v2} = k_{v2} K_{eq2} [H_2O]$ and $k'_{v3} = k_{v3} K_{eq3} [H_2O]$; K_{eq2} and K_{eq3} are the equilibrium constants for the formation of the ClOH···H_2O and H_2O···OH complexes, respectively. The computed values for K_{eq2} and K_{eq3} are given in Table S7 of the Supporting Information. k'_{v2} and k'_{v3} are effective rate constants that depend parametrically on the water concentration and can be directly compared to, k_{v1}, the rate constant of the naked reaction. Table 3 shows the collected k_{v1}/k'_{v2} and k_{v1}/k'_{v3} rates under different atmospheric conditions. The results show that the reaction beginning in the ClOH···H_2O + OH entrance channel is slower by 4 to 5 orders of magnitude than the reaction without water, whereas the predicted rate of the reaction between ClOH and H_2O···OH is 8.57×10^{-2} times smaller than the naked reaction at higher altitudes, around 12 km, but *almost two times faster at lower altitudes*.

To evaluate the atmospheric regions where the ClOH + OH + H_2O reaction will have significance, it is necessary to first estimate the amount of ClOH that is complexed with water under different atmospheric conditions. From the calculated equilibrium constant for ClOH···H_2O, displayed in Table S7 of the Supporting Information, and the water concentration at different heights displayed in Table 3, it is estimated that, at ground level, 0.63% of ClOH is in form of the ClOH···H_2O complex, and this value can increase up to 3.5% in humid conditions (i.e., 75% of relative humidity). This amount decreases rapidly with increasing altitude, down to 0.06% at 10 km.

As discussed earlier, hypochlorous acid (HOCl) is of great atmospheric interest as a reservoir of ClO_x and the role it plays in the loss of stratospheric ozone. Recently, the atmospheric importance of HOCl has been stressed after measurements of its atmospheric concentration. In the stratosphere, it is estimated that the maximum contribution to the total Cl abundance from HOCl is 0.192 ppbv at 35.5 km in the tropics, is 0.167 ppbv at 36.5 km in the midlatitudes, and is 0.098 ppbv at 37.5 km in the high latitudes; there is also a secondary peak at 23−25 km of 0.14 ppbv it the Antartic.[49−51] In the troposphere, HOCl has predicted peak concentrations ranging of a few ppt to several hundred in the marine boundary layer.[52] Therefore, it is interesting at this point to consider the possible atmospheric impact of the HOCl + OH reaction with and without water, and also whether the HOCl + OH (+ H_2O) reaction can be competitive with the photolysis rate of HOCl, 3×10^{-4} s^{-1}.[53] According to the results displayed in Table 3, under optimal conditions at 10 km with a [OH] = 2×10^6 molecules cm^{-3}, the lifetime of the HOCl + OH reaction becomes 1.45×10^{-7} s^{-1} and the lifetimes of the ClOH···H_2O + OH and ClOH + H_2O···OH reactions are 4.1×10^{-12} and 3.34×10^{-8} s^{-1} respectively, which suggest that the photolysis reaction is still dominant but that the HOCl + OH reaction cannot be ignored at lower altitudes. With an increase in altitude, into the stratosphere, there is both a decrease in the rate constant as well as a decrease in the concentration of water making the reaction with OH and H_2O insignificant compared to the photolysis rate at higher altitudes. In summary, these results suggest that at the lower troposphere and marine boundary layer there is a water effect on the ClOH + OH reaction.

4. SUMMARY AND CONCLUSIONS

Studying the effect that a single water molecule can have on the potential energy surface of the OH + HOCl reaction has revealed some interesting findings, particularly in the context of the OH + HOCl reaction without water. The reaction without water proceeds through two reaction channels, each one beginning with a five-member ring prereactive complex overcoming a transition-state barrier, which is effectively 2.0 and 1.4 kcal mol^{-1}, above the reactant level, before producing ClO and H_2O.

When water is added to the reaction, the resulting products do not change from that of the naked reaction forming ClO and H_2O. The formation of different products such as HCl are not predicted. However, the water molecule does impact the reaction. It can begin by collision of either HOCl···H_2O with OH or HO···H_2O with HOCl. The results from this study show that in both cases the reaction can proceed through the same elementary paths and that the potential energy surface is now much more complex yielding up to six different elementary reactions. In the HOCl···H_2O radical complex, the hydrogen atom of the HOCl moiety hydrogen bonds with the oxygen atom of the water molecule, hampering its ability to be abstracted by the hydroxyl radical. Thus, the first step of the reaction involves the formation of a three-body collision complex HOCl···H_2O···HO (**CR2**, with a binding energy of 2.17 kcal mol^{-1}) occurring previous to the formation of a three-body collision complex HOCl···HO···H_2O (**CR3**/**CR4**), in which the hydroxyl radical moiety interacts directly with the hydrogen atom of the HOCl to be abstracted. These complexes are quite stable (about 5 kcal mol^{-1}) and have an effective barrier of 1.65 kcal mol^{-1} above the HOCl···H_2O + OH reactants that must be overcome for the reaction to proceed. Note that this barrier is similar to the effective barrier of the reaction without water.

Another intriguing finding of this work is the three-body interchange reaction that can occur, that is HOCl + HO···H_2O → HOCl···H_2O + OH. This exchange reaction occurs through three different three-body HOCl·H_2O·HO collision complexes.

The rate constants computed for the reaction without water are in good agreement with the experimental values at 1 atm, between 200 and 350 K. The reaction between ClOH···H_2O and OH is predicted to be slower than the naked reaction by 4 to

5 orders of magnitude, whereas the reaction between ClOH and the $H_2O\cdots HO$ complex is predicted to be up to 2.2 times faster than the naked reaction at altitudes below 6 km. The branching ratios suggest that the major channel of the reaction is the formation of $ClOH\cdots H_2O + OH$ with a 99.5% yield and that the yield of ClO radicals at 0.5% is a small but contributing source of reactive chlorine.

The inclusion of a second water molecule produces a catalytic effect of 2.6 kcal mol^{-1} on the reaction. However, its atmospheric significance is very low because the atmospheric concentration of the $(H_2O)_2\cdots HO$ cluster is very small.

■ ASSOCIATED CONTENT

Supporting Information. Figure showing the most relevant geometrical parameters of the stationary points not shown in the text; tables with detailed kinetic parameters; table with relative energies for the reaction between HOCl and the $(H_2O)_2\cdots HO$ cluster; table with branching ratio for the reaction between ClOH and $H_2O\cdots HO$; table containing the equilibrium constants for the formation of the $ClOH\cdots H_2O$ and $H_2O\cdots HO$ complexes; tables containing the absolute energies computed for all stationary points; tables containing the corresponding Cartesian coordinates; and complete refs 6, 28, 30, 49, and 51. This material is available free of charge via the Internet at http://pubs.acs.org.

■ AUTHOR INFORMATION

Corresponding Author
jarqtc@cid.csic.es; francisc@purdue.edu

■ ACKNOWLEDGMENT

This research has been supported by the Spanish Dirección General de Investigación Científica y Técnica (DGYCIT, grant CTQ2008-06536/BQU) and by the Generalitat de Catalunya (Grant 2009SGR01472). The calculations described in this work were carried out at the Centre de Supercomputació de Catalunya (CESCA), CTI-CSIC, and the Rosen Center for Advanced Computing (RCAC).

■ REFERENCES

(1) Yung, Y. L.; Pinto, J. P.; Watson, R. T.; Sander, S. P. *J. Atmos. Sci.* **1980**, *37*, 339–353.
(2) Poulet, G.; Pirre, M.; Maguin, F.; Ramaroson, R.; Lebras, G. *Geophys. Res. Lett.* **1992**, *19*, 2305–2308.
(3) Garcia, R. R.; Solomon, S. *J. Geophys. Res.* **1994**, *99*, 12937–12951.
(4) Wofsy, S. C.; McElroy, M. B. *Can. J. Chem.* **1974**, *52*, 1582–1591.
(5) Solomon, S.; Garcia, R. R.; Rowland, F. S.; Wuebbles, D. J. *Nature* **1986**, *321*, 755–758.
(6) Wennberg, P. O.; et al. *Science* **1994**, *266*, 398–404.
(7) Stevens, P. S.; Anderson, J. G. *J. Phys. Chem.* **1992**, *96*, 1708–1718.
(8) Hansen, J. C.; Friedl, R. R.; Sander, S. P. *J. Phys. Chem. A* **2008**, *112*, 9229–9237.
(9) Ennis, C. A.; Birks, J. W. *J. Phys. Chem.* **1988**, *92*, 1119–1126.
(10) Atkinson, R.; Baulch, D. L.; Cox, R. A.; Hampson, R. F.; Kerr, J. A.; Rossi, M. J.; Troe, J. *J. Phys. Chem. Ref. Data* **1997**, *26*, 521–1011.
(11) Wang, L.; Liu, J. Y.; Li, Z. S.; Sun, C. C. *J. Comput. Chem.* **2004**, *25*, 558–564.
(12) Xu, Z. F.; Lin, M. C. *J. Phys. Chem. A* **2009**, *113*, 8811–8817.
(13) Vöhringer-Martinez, E.; Hansmann, B.; Hernandez, H.; Francisco, J. S.; Troe, J.; Abel, B. *Science* **2007**, *315*, 497–501.
(14) Luo, Y.; Maeda, S.; Ohno, K. *Chem. Phys. Lett.* **2009**, *469*, 57–61.
(15) Anglada, J. M.; Gonzalez, J. *Chemphyschem* **2009**, *10*, 3034–3045.
(16) Buszek, R. J.; Francisco, J. S. *J. Phys. Chem. A* **2009**, *113*, 5333–5337.
(17) Dunning, T. H. J. *J. Chem. Phys.* **1989**, *90*, 1007.
(18) Kendall, R. A.; Dunning, T. H.; Harrison, R. J. *J. Chem. Phys.* **1992**, *96*, 6796–6806.
(19) Becke, A. D. *J. Chem. Phys.* **1993**, *98*, 5648–5652.
(20) Ishida, K.; Morokuma, K.; Kormornicki, A. *J. Chem. Phys.* **1977**, *66*, 2153.
(21) Gonzalez, C.; Schlegel, H. B. *J. Phys. Chem.* **1990**, *94*, 5523.
(22) Cizek, J. *Adv. Chem. Phys.* **1969**, *14*, 35.
(23) Barlett, R. J. *J. Phys. Chem.* **1989**, *93*, 1963.
(24) Pople, J. A.; Krishnan, R.; Schlegel, H. B.; Binkley, J. S. *Int. J. Quant. Chem. XIV* **1978**, 545–560.
(25) Anglada, J. M.; Bofill, J. M. *Chem. Phys. Lett.* **1995**, *243*, 151–157.
(26) Bader, R. F. W. *Atoms in Molecules. A Quantum Theory*; Clarendon Press: Oxford, U. K., 1990.
(27) Truong, T. N.; Truhlar, D. G. *J. Chem. Phys.* **1990**, *93*, 1761.
(28) Frisch, M. J.;et al.; *Gaussian 03*, Revision C.01 ed.; Gaussian, Inc.: Wallingford, CT, 2004.
(29) Karlström, G.; Lindh, R.; Malmqvist, P.-Å.; Roos, B. O.; Ryde, U.; Veryazov, V.; Widmark, P.-O.; Cossi, M.; Schimmelpfennig, B.; Neogrady, P.; Seijo, L. *Comput. Mater. Sci.* **2003**, *28*, 222.
(30) Corchado, J. C.; et al. *POLYRATE*, version 9.3 ed.; University of Minnesota: Minneapolis, 2002.
(31) Bader, R. F. W. Accessed May 2002; http://www.chemistry.mcmaster.ca/aimpac.
(32) Shaftenaar, G.; Noordik, J. H. *J. Comput.-Aided Mol. Design* **2000**, *14*, 123–134.
(33) Ruscic, B.; Wagner, A. F.; Harding, L. B.; Asher, R. L.; Feller, D.; Dixon, D. A.; Peterson, K. A.; Song, Y.; Qian, X. M.; Ng, C. Y.; Liu, J. B.; Chen, W. W. *J.Phys. Chem. A* **2002**, *106*, 2727–2747.
(34) Matusgh, M. H.; Nguyen, M. T.; Dixon, D. A.; Peterson, K. A.; Francisco, J. S. *J. Phys. Chem. A* **2008**, *112*, 9623–9627.
(35) Chase, M. W.; Davies, C. A.; Downey, J. R.; Frurip, D. J.; McDonald, R. A.; Syverud, A. N. *J. Phys. Chem. Ref. Data* **1985**, *14*, 1–926.
(36) Barnes, R. J.; Sinha, A. *J. Chem. Phys.* **1997**, *107*, 3730–3733.
(37) Dibble, T. S.; Francisco, J. S. *J. Phys. Chem.* **1995**, *99*, 1919–1922.
(38) Allodi, M. A.; Dunn, M. E.; Livada, J.; Kirschner, K. N.; Shields, G. C. *J. Phys. Chem. A* **2006**, *110*, 13283–13289.
(39) Cooper, P. D.; Kjaergaard, H. G.; Langford, V. S.; McKinley, A. J.; Quickenden, T. I.; Schofield, D. P. *J. Am. Chem. Soc.* **2003**, *125*, 6048–6049.
(40) Engdahl, A.; Karlstrom, G.; Nelander, B. *J. Chem. Phys.* **2003**, *118*, 7797–7802.
(41) Ohshima, Y.; Sato, K.; Sumiyoshi, Y.; Endo, Y. *J. Am. Chem. Soc.* **2005**, *127*, 1108–1109.
(42) Olivella, S.; Anglada, J. M.; Sole, A.; Bofill, J. M. *Chem.—Eur. J.* **2004**, *10*, 3404–3410.
(43) Anglada, J. M. *J. Am. Chem. Soc.* **2004**, *126*, 9809–9820.
(44) Gonzalez, J.; Caballero, M.; Aguilar-Mogas, A.; Torrent-Sucarrat, M.; Crehuet, R.; Solé, A.; Giménez, X.; Olivella, S.; Bofill, J. M.; Anglada, J. M. *Theor. Chem. Acc.* Published online at 30 September 2010.
(45) Castleman, A. W., Jr.; Jena, P. *Proc. Natl. Acad Sci. U.S.A.* **2006**, *103*, 10552–3.
(46) Raff, J. D.; Njegic, B.; Chang, W. L.; Gordon, M. S.; Dabdub, D.; Gerbera, R. B.; Finlayson-Pitts, B. J. *Proc. Natl. Acad. Sci. U.S.A.* **2009**, *106*, 13647–13654.

(47) Miller, W. H. *J. Chem. Phys.* **1976**, *65*, 2216–2223.
(48) Hu, W. P.; Truhlar, D. G. *J. Am. Chem. Soc.* **1996**, *118*, 860–869.
(49) Nassar, R.; et al. *J. Geophy. Res.* **2006**, *111*, D22312.
(50) von Clarmann, T.; Glatthor, N.; Grabowski, U.; Hopfner, M.; Kellmann, S.; Linden, A.; Tsidu, G. M.; Milz, M.; Steck, T.; Stiller, G. P.; Fischer, H.; Funke, B. *J. Geophys. Res.* **2006**, *111*, D05311.
(51) Fischer, H.; et al. *Atmos. Chem. Phys.* **2008**, *8*, 2151–2188.
(52) Caldwell, T. E.; Foster, K. L.; Benter, T.; Langer, S.; Hemminger, J. C.; Finlayson-Pitts, B. J. *J. Phys. Chem. A* **1999**, *103*, 8231–8238.
(53) DeMore, W. B.; Sander, S. P.; Golden, D. M.; Hampson, R. F.; Kurylo, M. J.; Howard, C. J.; Ravishankara, A. R.; Kolb, C. E.; Molina, M. J. *JPL Publication 97−4*; Jet Propulsion Laboratory, CA, 1997.
(54) *Photochemistry of Planetary Atmospheres*; Yung, Y. L.; Demore, W. B., Eds.; Oxford Univ. Press: Oxford, 1999.
(55) NASA, accessed December 2010; http://www.grc.nasa.gov/WWW/K-12/airplane/atmosi.html

■ NOTE ADDED AFTER ASAP PUBLICATION

The version of this article published ASAP February 14, 2011, had a typographical error in the second set of equations shown in the Introduction. The equation was corrected February 18, 2011.